Sizing of a Heliostats Field of a Mini Solar Tower in Adrar Region (Algeria)

Mohamed Douak
Laboratory of Applied Energetic Physics, Faculty of Material Sciences, Kasdi Merbah Ouargla University, Algeria
douakmohamed@gmail.com

Abdelatif Gadoum
LRPPS Laboratory, Faculty of Mathematics and Material Sciences, Kasdi Merbah Ouargla University, Algeria | Electrical Engineering and Renewable Energies Laboratory, Electrical Engineering Department, Chlef University, Algeria
gdabdelatif@gmail.com (corresponding author)

Zaroual Aouachria
Applied Energy Physics Laboratory (LPEA), Department of Materials Science, Batna 1 University, Algeria
aouachria2001@gmail.com

Received: 20 February 2025 | Revised: 31 March 2025 | Accepted: 2 April 2025

 DOI: https://doi.org/10.48084/etasr.10647

ABSTRACT

This study describes the design of a 10-kW solar tower for the Adrar region in southwest Algeria. The heliostats were arranged according to an offset radial pattern, safety distances between adjacent heliostats, surface density criteria, and the blocking factor of solar rays. The heliostat field was designed for a tower height of 18 m with an optical efficiency of 69%, and individual heliostat surfaces of 2.25 m². To model the optical behavior of the heliostat field and receiver, a code in FORTRAN was developed. The results show that a reflective surface of 81 m² of the 36 heliostats is necessary to reach the target power of 10 kW. This approach offers a comprehensive method for heliostat field design, optimizing solar radiation collection, and minimizing losses due to shading and blocking. The developed simulation tool also allows for quick evaluation and adjustment of system parameters, facilitating the design process for similar solar tower systems in other regions.

Keywords-heliostats; sizing; radial staggered field; heliostat field efficiency; solar tower

I. INTRODUCTION

Solar energy, a renewable and abundant resource, plays a critical role in mitigating climate change by reducing greenhouse gas emissions while providing a sustainable and reliable alternative to fossil fuels [1-5].

Solar thermodynamics refers to all technologies that convert radiated energy from the sun into heat at temperatures high enough to create high-performance thermodynamic cycles. To reach these temperatures, radiant energy must be collected and concentrated by an appropriate system. This technology is designed to couple a Brayton, Rankine, or both thermodynamic cycles using steam, gas, or air to an electric generator for electrical power generation [1].

Optimizing the heliostat field is crucial because it constitutes the primary cost component of a solar thermal power plant. This component represents 50% of the plant's total cost and 40% of its energy losses [2]. Additionally, the optical quality of heliostats significantly affects the field efficiency and, consequently, the overall plant performance. Therefore, the ongoing objective is to reduce manufacturing costs and improve optical quality. Hence, to define the optical efficiency of the heliostat field, it is necessary to adopt an economic and precise approach. The design of a heliostat field depends on several factors, such as the tower height, receiver shape and inclination, latitude of the location, meteorological data, and topography of the terrain. In addition, fields are varied: they can be circular [3, 4], symmetrical oriented towards the north, asymmetrical with heliostats arranged in corncobs, or offset radially [6], spiral [7], and standard biomimetic heliostatic fields [8-10]. When heliostats are placed closer together, blockage and shading losses increase, but the costs associated with land and wiring can decrease. All these constraints make the design of a heliostat field a complex task. To overcome these problems, several codes have been developed [11-13].

The current study provides a comprehensive and practical approach to solar tower design, particularly during the design phase. Given the challenges and high costs associated with experimental testing, this computational methodology offers a more accessible and cost-effective alternative for sizing and optimizing heliostat fields. The ability to simulate and model the system performance without the need for physical prototypes or large-scale trials is crucial for advancing the design of solar power systems.

The present study introduces an original design for a 10-kW mini solar tower, specifically tailored to the unique solar and environmental conditions of the Adrar region, addressing the gap in small-scale solar thermal systems that are often overlooked in favor of larger-scale studies. Its novelty lies in the custom FORTRAN code, which can be used for cost-effective optical modeling and optimized offset radial heliostat field layout, enhancing practicality for resource-limited settings. The study's importance stems from its focus on decentralized energy solutions, offering a replicable and scalable framework that leverages Adrar's high solar potential to support Algeria's renewable energy goals in arid, remote areas.

II. SYSTEM DESCRIPTION

The diagram in Figure 1 illustrates the flow of energy within the system, starting with the hot air collector, which preheats the air before it enters the receiver. The receiver absorbs the concentrated solar radiation reflected from the heliostat field and further heats the air to high temperatures. The heated air is then directed to a turbine, where its thermal energy is converted into mechanical energy. The mechanical energy produced by the turbine is harnessed to drive an alternator, which, in turn, generates electrical power. Under optimal solar conditions, specifically at solar noon, when sunlight is at its peak intensity, the system is designed to produce a total of 10 kW of electrical power. This power output is essential for the efficient operation of the solar tower, ensuring that the system meets its performance targets while maximizing energy conversion during periods of peak solar irradiation.

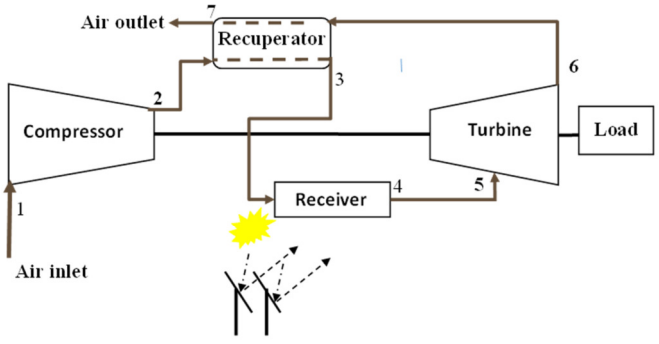

Fig. 1. Schematic representation of the solar tower.

III. SIZING THE REFLECTIVE SURFACE OF THE HELIOSTAT FIELD

To determine the reflecting surface area required for the heliostat field, the methodology outlined in Figure 2 was followed. This approach begins by calculating the thermal power necessary to generate the desired electrical output from the turbine. The nominal power and efficiency of the turbine were used to estimate the amount of thermal energy that needed to be captured and converted into electricity. Specifically, the thermal power is derived by considering the electrical output of the turbine and the efficiency of the energy conversion process, which accounts for losses in both the mechanical and electrical stages.

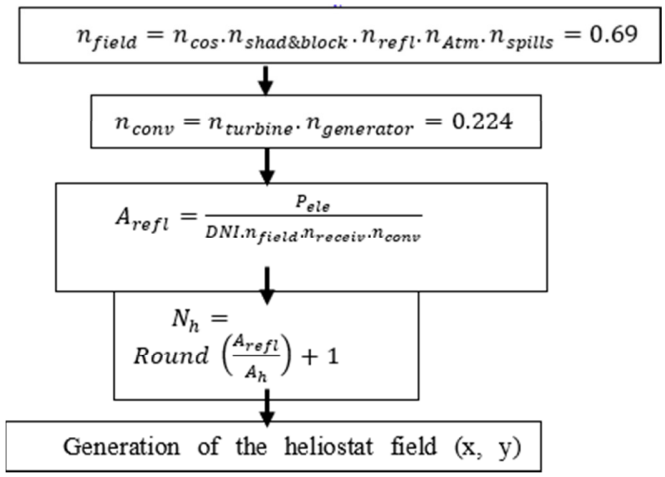

Fig. 2. Sizing methodology for the solar tower.

By determining the required thermal power, the present study can then establish the appropriate reflecting surface area of the heliostat field needed to concentrate sufficient solar radiation onto the receiver to achieve the desired power generation. This method ensures that the heliostat field is adequately sized to meet the system's energy demands under optimal solar conditions.

The efficiency of the heliostat field is estimated using:

$$n_{field} = n_{cos}.n_{shad\&block}.n_{refl}.n_{Atm}.n_{spills} \quad (1)$$

where η_{cos}, η_{Atm}, η_{refl}, η_{spills}, and $\eta_{shad\&block}$ represent the efficiencies of cosine, atmospheric attenuation, reflective, spillage, shading, and blocking, respectively. The values of these parameters are given in Table I.

TABLE I. SOLAR TOWER EFFICIENCIES

η_{cos}	η_{Atm}	η_{refl}	η_{spill}	$\eta_{shad\&blok}$	η_{receiv}	$\eta_{turbine}$
0.88	0.95	0.86	0.97	0.99	0.80	0.25

The reflective surface can be deduced by:

$$A_{refl} = \frac{P_{ele}}{DNI.n_{field}.n_{receiv}.n_{conv}} \quad (2)$$

where DNI is the Direct Normal Irradiance (W/m²), $\eta_{turbine}$, $\eta_{generator}$ are the efficiencies of the turbine and the generator,

respectively, and η_{conv} is the efficiency of the receiver, which is defined by:

$$n_{conv} = n_{turbine} \cdot n_{generator} \quad (3)$$

The values of these parameters are given in Table I.

The reflective surface corresponding to the N_h heliostat is:

$$N_h = Round\left(\frac{A_{refl}}{A_h}\right) + 1 \quad (4)$$

Once the configuration of the installation is obtained, the thermal power concentrated on the receiver can be evaluated using:

$$Q_{in-rec} = DNI.n_{field}.A_m.N_h \quad (5)$$

The electrical power produced by the solar tower conversion system is given by:

$$P_{elec} = n_{receptor} \cdot n_{conv} \cdot Q_{in-rec} \quad (6)$$

IV. MATHEMATICAL MODELING

A radially offset field was chosen to increase the efficiency of the system, while minimizing blocking and shading losses [13-15]. The offset field was placed north of the tower. The mathematical model of the heliostat field was adopted from [14]. The characteristic diameter of the sphere was determined using:

$$DM = (\sqrt{1+f^2} + ds)l_m \quad (7)$$

where f is the ratio of the width to the length of the heliostat and is given by:

$$f = \frac{w_m}{l_m} \quad (8)$$

where ds stands for the inter-heliostat safety factor, and its minimum value is given by:

$$ds_{min} = 2f - \sqrt{1+f^2} \quad (9)$$

Thus, the minimum value of the characteristic diameter of the sphere is determined by:

$$DM_{min} = 2W_m \quad (10)$$

As shown in Figure 3, heliostats with the same azimuthal spacing can be classified into the same groups. The first group is the essential ring group.

The angular direction unit (γ_j) represents the angle between the distribution axes. In a ring, the azimuthal angle of the first group is constant, and is defined by:

$$\gamma_j = \frac{DM}{2R_{0,j}} \quad (11)$$

where $R_{i,j}$ is the radius of ring i in group j.

The angular direction is the angle between the north axis and the distribution axes, which is determined by:

$$\psi = \pm n\gamma_j \quad (12)$$

where n= 0, 2, 4, 6, …, for essential rings, n=1, 3, 5, 7, … for staggered rings, and + is for NE half field and – for NW half field.

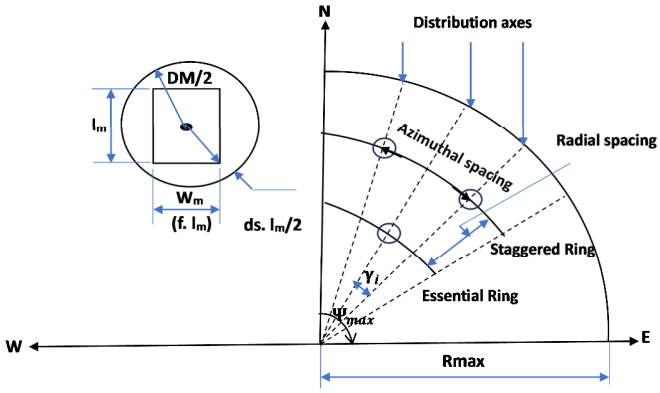

Fig. 3. Distribution axes.

The radial spacing is defined as the radius of each ring in the field and is determined by the type of ring. For the first ring it can be expressed by:

$$R_{0,j} = R_{min} = 0.6H_t \quad (13)$$

For the other rings, it is given by [15, 16]:

$$R_{i+1,j} = R_{i,j} + DMcos30°cos\beta_L;\ i = 0,1,2,\ldots \quad (14)$$

where β_L is the terrain slope rising from the tower, as depicted in Figure 4.

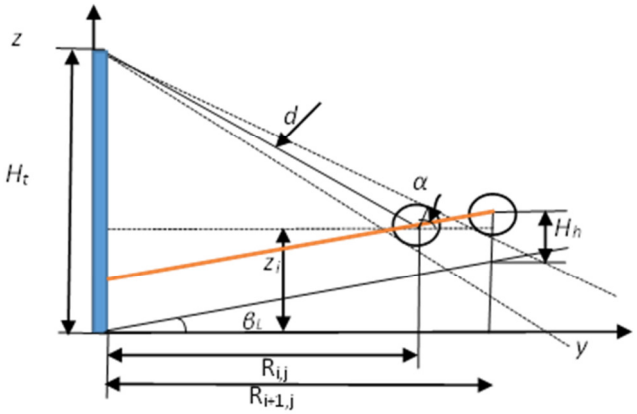

Fig. 4. Radius without blocking

The maximum radial spacing should satisfy the following condition [16]:

$$\Delta R_{max} = \frac{DMcos\beta_L}{cos\alpha} \quad (15)$$

where α is determined from Figure 4 as:

$$a = arcsin\left(\frac{DM}{2d}\right) + arcsin\left(\frac{R_{ij}}{d}\right) - \beta_L \quad (16)$$

According to Figure 4, the distance of each heliostat from the tower receiver (d) is determined using the Pythagorean theorem:

$$d = \sqrt{{R_{ij}}^2 + (H_t\text{-}Z_i)^2} \quad (17)$$

The Z_i is given by:

$$Z_i = R_{ij}tan\beta_L + H_h \quad (18)$$

Once the angular direction of the heliostat and the radius of the ring to which it belongs are fixed, the center coordinates of the heliostat can be determined according to:

$$x_m = R_{ij}sin(\psi)$$
$$y_m = R_{ij}cos(\psi) \quad (19)$$
$$Z_m = R_{ij}tan\beta_L + H_h$$

V. RESULTS AND DISCUSSION

A custom FORTRAN code was developed to model the optical behavior of the entire heliostat field and the solar tower receiver. This code simulates the reflection of solar radiation by the heliostats and the subsequent concentration of that energy onto the receiver, accounting for various factors, such as heliostat positioning, orientation, and optical characteristics. The program computes the precise position of each heliostat within the field, ensuring the accurate modeling of the reflection patterns and energy distribution. The simulation parameters used to configure the model, including the key geometric and optical characteristics of the heliostats and the receiver, are illustrated in Figures 3 and 4, and are provided in Table II. These parameters are crucial for understanding the performance of the heliostat field and optimizing the overall efficiency of the solar tower system.

TABLE II. DESIGN SPECIFICATIONS OF DIFFERENT PARAMETERS

Parameter	symbol	value
Heliostat length	l_m	1.5 m
Heliostat width	w_m	1.5 m
Height of the heliostat center from the base	H_h	1 m
Inter heliostat safety factor	ds	0.1 m
Tower height	H_t	18 m
Terrain slope rising away from the tower	β_L	30°
Maximum angular direction (opening angle of the field)	Ψ_{max}	45°
Ratio of reflective area to total area of a heliostat	f_a	1

TABLE III. HELIOSTAT FIELD SIZING

Parameter	Symbol	Value
Reflecting surface	A_{ref}	81 m^2
Total surface of heliostat	A_h	2.25 m²
Total Number of heliostats	N_h	36
Minimal radius of heliostat field	R_{min}	10.8 m
Maximal radius of heliostat field	R_{max}	17.17
Azimuthal angle	γ_{ij}	5.629°
Characteristic diameter	DM	2.12 m
Radial spacing	ΔR_{min}	1.6 m
Number of heliostats in essential ring	N_{m1}	7 heliostats
Number of heliostats in staggered ring	N_{m2}	8 heliostats
Number of rings	N_{an}	5 rings

According to the values shown in Table III, and under a solar radiation of 1000 W/m^2 received on the heliostat field, the reflective area required to produce 10 kW is 81 m^2, which corresponds to 36 heliostats of 2.25 m^2 each. In addition, at a height of 18 m from the receiver, the minimum and maximum heliostat field radius should be 10.8 m and 17.17 m, respectively. The azimuth spacing has a value of 2.12 m. The heliostats were distributed on five original rings, separated by a radial spacing offset between them of ΔR_{min} = 1.6 m. Tables II and III outline all key parameters and design considerations for the heliostat field in the solar tower system, which are critical for optimizing the efficiency of solar energy capture and power generation.

Table IV presents the detailed configuration of the heliostat field, specifying the radius, height, number of heliostats, and tilt angle for each ring of heliostats. These specifications are particularly important for fine-tuning the system design, as the optimal arrangement and tilt angle of the heliostats are key to maximizing the reflection of solar radiation and minimizing the losses. The detailed distribution of heliostats across different rings ensures efficient light capture at various sun angles, directly affecting the system's overall energy output and operational efficiency.

TABLE IV. DETAILED HELIOSTAT FIELD SIZING

Ring	Radius (m)	High (m)	Number of heliostats	Tilt angle of heliostatαh (0C)
1	10.8	7.23	7	19
2	12.4	8.15	8	8.3
3	14	9.06	7	32.8
4	15.6	9.98	8	38.46
5	17.17	10.9	6	43.4

Once the angular direction of the heliostat and the radius of the ring to which it belongs are fixed, the center coordinates of the heliostat can be determined using (19). The heliostat field shown in Figure 5 is arranged in concentric rings with varying radii, and the heliostats are placed along these rings at specific angular intervals influenced by the radial spacing and tilt angles.

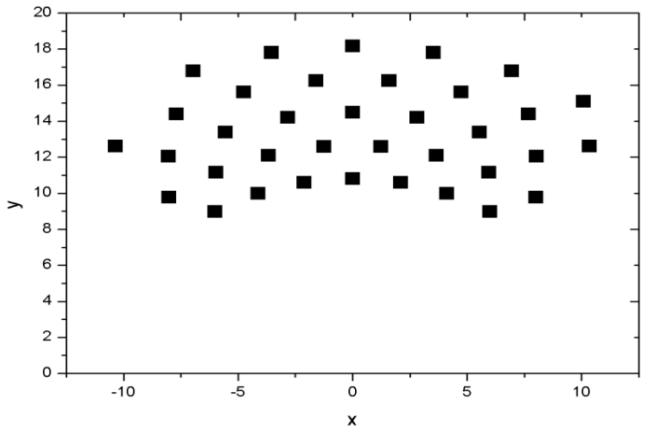

Fig. 5. Position of the heliostats.

Figure 6 presents the direct DNI received on a unit plane on April 15. The graph highlights the variation in solar irradiance throughout the day, with the maximum DNI reaching 832 W/m². This value represents the highest level of solar energy incident per unit area and is indicative of the optimal solar exposure for that particular day. The distribution and intensity

of the DNI throughout the day reflect the influence of factors, such as the solar zenith angle, atmospheric conditions, and time of day.

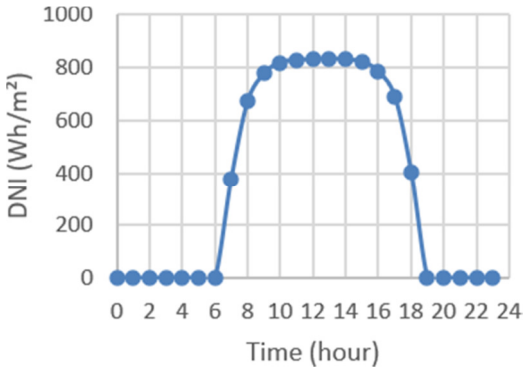

Fig. 6. Direct normal solar irradiance received.

Figure 7 illustrates the total flux reflected by all heliostats and subsequently received by the receiver of the solar tower. The plot demonstrates the temporal variation in the reflected flux throughout the day, with the peak flux reaching approximately 800 Wh/m² around midday, specifically between 12:00 and 13:00. This maximum flux value corresponds to the optimal alignment of the heliostats, where the reflected solar energy is focused most efficiently on the receiver. The distribution of the flux over time is influenced by factors, such as the position of the sun, heliostat orientation, and atmospheric conditions, which together determine the overall energy concentration received by the receiver at any given moment.

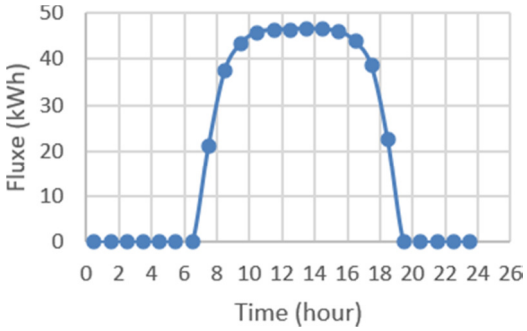

Fig. 7. Solar flux received by the receiver.

Figure 8 displays the electrical power output generated by the solar tower throughout the day. The graph highlights the temporal variation in power production, with the maximum output reaching 8.34 kW at around midday, specifically between 12:00 and 13:00. This peak power production is a result of the optimal solar irradiance and the efficient operation of the system, since both the DNI and the reflected flux from the heliostats are maximized during this period. The electrical power produced by the solar tower is directly influenced by factors, such as solar insolation, the alignment of the heliostats, and the performance of the power conversion system, all of which contribute to the system's efficiency in converting solar energy into electrical power at different times of the day.

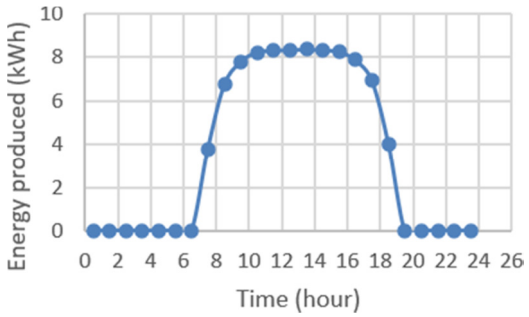

Fig. 8. Electric power produced.

VI. CONCLUSIONS

This study employed a simplified graphical method for arranging heliostat fields, specifically designed to avoid blocking effects, which is particularly useful during the preliminary design phase of solar tower systems. A FORTRAN-based program was developed to facilitate the design process, enabling the visualization of the heliostat field layout on a computer screen. The program also allows the storage of output data, including heliostat identification numbers and their corresponding location coordinates, thereby streamlining the design and analysis workflow.

Additionally, the sizing of the heliostat field for a 10-kW mini solar tower in the Adrar region was thoroughly analyzed. The results exhibited that a total reflecting surface area of 81 m², composed of 36 heliostats with an individual area of 2.25 m² each, is necessary to meet the 10-kW electrical power generation target. Furthermore, under optimal conditions, with a Direct Normal Irradiance (DNI) of 1 kW/m² on April 15, the system achieved a maximum power output of 56 kW. These findings provide valuable insights into the design and performance characteristics of small-scale solar tower systems, highlighting the importance of the heliostat field configuration and solar irradiance conditions in determining system efficiency.

This study provides a cost-effective and efficient approach to heliostat field design using a computational model, which avoids the need for costly experimental testing. This methodology enables the accurate sizing and optimization of solar tower systems during the preliminary design phase, contributing to more rapid and reliable assessments of system performance.

REFERENCES

[1] H. H. H. de Silva, D. K. J. S. Jayamaha, and N. W. A. Lidula, "Power Quality Issues Due to High Penetration of Rooftop Solar PV in Low Voltage Distribution Networks: A Case Study," in *2019 14th Conference on Industrial and Information Systems (ICIIS)*, Kandy, Sri Lanka, Sep. 2019, pp. 395–400, https://doi.org/10.1109/ICIIS47346.2019.9063322.

[2] T. Eldamaty, A. G. Ahmed, and M. M. Helal, "GIS-Based Multi Criteria Analysis for Solar Power Plant Site Selection Support in Mecca," *Engineering, Technology & Applied Science Research*, vol. 13, no. 3, pp. 10963–10968, Jun. 2023, https://doi.org/10.48084/etasr.5927.

[3] A. K. M. Ashikuzzaman and S. Adnan, "Optical efficiency comparison of circular heliostat fields: Engender of hybrid layouts," *Renewable Energy*, vol. 178, pp. 506–519, Nov. 2021, https://doi.org/10.1016/j.renene.2021.06.083.

[4] Md. R. Islam, Md. T. Aziz, M. Alauddin, Z. Kader, and Md. R. Islam, "Site suitability assessment for solar power plants in Bangladesh: A GIS-based analytical hierarchy process (AHP) and multi-criteria decision analysis (MCDA) approach," *Renewable Energy*, vol. 220, Jan. 2024, Art. no. 119595, https://doi.org/10.1016/j.renene.2023.119595.

[5] S. N. Shorabeh, M. K. Firozjaei, O. Nematollahi, H. K. Firozjaei, and M. Jelokhani-Niaraki, "A risk-based multi-criteria spatial decision analysis for solar power plant site selection in different climates: A case study in Iran," *Renewable Energy*, vol. 143, pp. 958–973, Dec. 2019, https://doi.org/10.1016/j.renene.2019.05.063.

[6] H. A. Hadi, A. Kassem, H. Amoud, and S. Nadweh, "Improve power quality and stability of grid - Connected PV system by using series filter," *Heliyon*, vol. 10, no. 21, Nov. 2024, Art. no. e39757, https://doi.org/10.1016/j.heliyon.2024.e39757.

[7] S. Boubaker, S. Kamel, and M. Kchaou, "Prediction of Daily Global Solar Radiation using Resilient-propagation Artificial Neural Network and Historical Data: A Case Study of Hail, Saudi Arabia," *Engineering, Technology & Applied Science Research*, vol. 10, no. 1, pp. 5228–5232, Feb. 2020, https://doi.org/10.48084/etasr.3278.

[8] Y. Kassem, H. Camur, M. T. Adamu, T. Chikowero, and T. Apreala, "Prediction of Solar Irradiation in Africa using Linear-Nonlinear Hybrid Models," *Engineering, Technology & Applied Science Research*, vol. 13, no. 4, pp. 11472–11483, Aug. 2023, https://doi.org/10.48084/etasr.6131.

[9] A. Alghamdi, J. Jose Ponnore, A. M Hassan, S. Alqahtani, S. Alshehery, and A. E Anqi, "Exergy-economic analysis of a hybrid combined supercritical Brayton cycle-organic Rankine cycle using biogas and solar PTC system as energy sources," *Case Studies in Thermal Engineering*, vol. 50, no. September, 2023, Art. no. 103484, https://doi.org/10.1016/j.csite.2023.103484.

[10] S. M. Besarati and D. Yogi Goswami, "A computationally efficient method for the design of the heliostat field for solar power tower plant," *Renewable Energy*, vol. 69, pp. 226–232, Sep. 2014, https://doi.org/10.1016/j.renene.2014.03.043.

[11] Z.-H. Cheng, J.-J. Zhang, J. Pan, B.-T. Cao, and L.-X. Xu, "Field Optimization of Tower Solar Heliostatic Mirror Based on Ant-Field Reflector Algorithm and Particle Ray Tracing Optimization," in *2024 International Conference on Wavelet Analysis and Pattern Recognition (ICWAPR)*, Miyazaki, Japan, Sep. 2024, pp. 1–6, https://doi.org/10.1109/ICWAPR63074.2024.10870499.

[12] M. Gadalla and M. Saghafifar, "Thermo-economic and comparative analyses of two recently proposed optimization approaches for circular heliostat fields: Campo radial-staggered and biomimetic spiral," *Solar Energy*, vol. 136, pp. 197–209, 2016, https://doi.org/10.1016/j.solener.2016.07.006.

[13] D.-T. Duan *et al.*, "Large-Scale Heliostat Field Optimization for Solar Power Tower System Using Matrix-Based Differential Evolution," *IEEE Transactions on Artificial Intelligence*, pp. 1–14, 2025, https://doi.org/10.1109/TAI.2025.3545813.

[14] M. Haris *et al.*, "Genetic algorithm optimization of heliostat field layout for the design of a central receiver solar thermal power plant," *Heliyon*, vol. 9, no. 11, Nov. 2023, Art. no. e21488, https://doi.org/10.1016/j.heliyon.2023.e21488.

[15] O. Behar, A. Khellaf, and K. Mohammedi, "A review of studies on central receiver solar thermal power plants," *Renewable and Sustainable Energy Reviews*, vol. 23, no. July, pp. 12–39, Jul. 2013, https://doi.org/10.1016/j.rser.2013.02.017.

[16] S. Boudaoud, A. Khellaf, K. Mohammedi, and O. Behar, "Thermal performance prediction and sensitivity analysis for future deployment of molten salt cavity receiver solar power plants in Algeria," *Energy Conversion and Management*, vol. 89, pp. 655–664, Jan. 2015, https://doi.org/10.1016/j.enconman.2014.10.033.